

## Rocking Ratchets in Two-Dimensional Josephson Networks: Collective Effects and Current Reversal

Verónica I. Marconi

*Institut de physique, Université de Neuchâtel, CH-2000 Neuchâtel, Switzerland*

(Received 30 June 2006; published 25 January 2007)

A detailed numerical study on the directed motion of ac-driven vortices and antivortices in 2D Josephson junction arrays with an asymmetric periodic pinning potential is reported. dc-voltage rectification shows a strong dependence on vortex density as well as an inversion of the vortex flow direction with ac amplitude for a wide range of vortex density around  $f = 1/2$  ( $f = Ha^2/\Phi_0$ ), in good agreement with recent experiments by Shalóm and Pastoriza [Phys. Rev. Lett. **94**, 177001 (2005)]. The study of vortex structures, spatial and temporal correlations, and vortex-antivortex pairs formation gives insight into a purely collective mechanism behind the current reversal effect.

DOI: [10.1103/PhysRevLett.98.047006](https://doi.org/10.1103/PhysRevLett.98.047006)

PACS numbers: 74.81.Fa, 74.25.Qt, 85.25.Cp

Ratchet systems constitute a vast subject of present interest, extensively studied from biology to a wide spectrum of fields in physics [1–5]. Very recently, promising applications in micro–nanotechnology have motivated a huge amount of additional works, mainly regarding the controlled motion of nanoparticles, colloids, electrons, or magnetic flux quanta. The main characteristic of these systems is their ability to transport particles with a nonzero drift velocity in the absence of any net macroscopic force. The simplest realization of this idea is the rectification of an ac-driven single particle motion in an asymmetric periodic potential or ratchet potential, known as a *rocking ratchet*. Ratchet effect in superconductors (SC) has been, in particular, an attractive subject of study since the proposal of using it to remove undesirable trapped vortices producing noise in SC devices [6]. Notably, several designs of asymmetric pinning potentials for the motion of flux quanta have been recently realized, such as dots–antidots arrays of pinning sites in SC films [7]. Even more, ratchet designs without spatial asymmetry have been successfully achieved in layered SC [8]. Small Josephson junction (JJ) systems were investigated as well: SQUIDs [9], 1D ladders [10,11], long JJ [12], and quasi-1D quantum JJA [13]. In particular, on classical JJA, the first design of a device for kinks motion rectification was proposed [10] and measured [11] in 1D.

Large 2D JJA, which are excellent systems to study statistical mechanics experimentally [14] and where collective effects could play a relevant role, had not been studied until very recently. Rectification experiments on 2D JJA were reported by Shalóm and Pastoriza [15]. They modulated the distance between the SC islands thus generating a ratchet potential for vortex motion. dc-voltage rectification was then clearly observed and its intriguing features, such as a nontrivial dependence on both the applied ac current and vortex density, and an inversion of the vortex flow direction, prompt further investigation. The aim of this Letter is to interpret such experiments and understand the role of collective effects. We show numerically that the

overdamped RSJ model for large 2D JJA with asymmetrically modulated critical currents, reproduces successfully the experiments [15] and allows for a detailed characterization of the device useful for performance enhancement and future experiments. In addition, a complete study of the vortex dynamics gives insight into a nontrivial collective mechanism behind the current reversal (CR) effect.

We study the overdamped vortex dynamics in square 2D asymmetrically modulated JJA using the resistively shunted junction (RSJ) model [16] and solving numerically the superconducting phase dynamics. The current flowing in the junction between two superconducting islands is the sum of the Josephson supercurrent and the normal current:  $I_\mu(\mathbf{n}) = I_0 \sin\theta_\mu(\mathbf{n}) + \frac{\Phi_0}{2\pi c R_N} \frac{\partial \theta_\mu(\mathbf{n})}{\partial t} + \eta_\mu(\mathbf{n}, t)$ , where  $I_0$  is the critical current of the junction between the two superconducting islands sited in  $\mathbf{n}$  and  $\mathbf{n} + \boldsymbol{\mu}$  on a square lattice [ $\mathbf{n} = (n_x, n_y)$ ,  $\boldsymbol{\mu} = \hat{\mathbf{x}}, \hat{\mathbf{y}}$ ],  $\theta_\mu(\mathbf{n}) = \theta(\mathbf{n} + \boldsymbol{\mu}) - \theta(\mathbf{n}) - A_\mu(\mathbf{n})$  the gauge invariant phase difference with  $A_\mu(\mathbf{n}) = \frac{2\pi}{\Phi_0} \int_{\mathbf{n}a}^{(\mathbf{n}+\boldsymbol{\mu})a} \mathbf{A} \cdot d\mathbf{l}$ ,  $\Phi_0$  the flux quantum,  $a$  the lattice parameter, and  $R_N$  the normal state resistance. Under a magnetic field  $H$ , we have  $\Delta_\mu \times A_\mu(\mathbf{n}) = 2\pi f$ ,  $f = Ha^2/\Phi_0$  being the frustration parameter, a measure of the vortex density. The Langevin noise term  $\eta_\mu$  models the contact with a thermal bath at temperature  $T$  and satisfies  $\langle \eta_\mu(\mathbf{n}, t) \eta_{\mu'}(\mathbf{n}', t') \rangle = \frac{2k_B T}{R_N} \delta_{\mu, \mu'} \delta_{\mathbf{n}, \mathbf{n}'} \delta(t - t')$ . The ratchet potential for vortices is introduced by modulating the critical currents  $I_0 = E_J \Phi_0 / 2\pi$ ,  $E_J$  being the Josephson coupling energy between islands. We consider a sawtooth modulation  $I_0(n_x)$  increasing linearly from  $I_{0_{\min}}$  to  $I_{0_{\max}}$  within each period  $p$  as an approximation to the experimental modulation. The ratchet potential amplitude is then measured by  $\Delta U \propto \Delta I_0 = (I_{0_{\max}} - I_{0_{\min}})$ . The system is driven by  $I_{\text{ext}} = I_{\text{ac}} \sin(2\pi \omega_{\text{ac}} t)$  in the  $\hat{\mathbf{y}}$  direction. Periodic boundary conditions in both directions are taken (see model details in [17]). The dynamical equations for the superconducting phases are obtained after considering conservation of the current in each node. The resulting set of Langevin equations are solved using a second order

Runge-Kutta algorithm with time step  $\Delta t = 0.1\tau_J$  ( $\tau_J = 2\pi cR_N\bar{I}_0/\Phi_0$ , where  $\bar{I}_0$  is the averaged critical current) and integration time  $2 \times 10^6\tau_J$  after the equilibration transient. We calculate: mean dc voltage as  $\langle V_{dc} \rangle = -\langle d\theta_y(\mathbf{n})/dt \rangle$  [17] vs both  $I_{ac}$  and  $f$  where  $\langle \dots \rangle$  stands for both time and space average; vorticity at the plaquette  $\tilde{\mathbf{n}} = (n_x + 1/2, n_y + 1/2)$ , as  $b(\tilde{\mathbf{n}}) = -\Delta_\mu \times \text{nint}[\theta_\mu(\mathbf{n})/2\pi]$  [18] ( $\text{nint}[\dots]$  being the nearest integer function). Currents are normalized by  $\bar{I}_0$ , voltages by  $R_N\bar{I}_0$ , temperature by  $\bar{E}_J/k_B$  and frequencies by  $(\tau_J)^{-1}$ . Most of the results shown are (except indication) for  $p = 8$ ,  $I_{0\min} = 0.5\bar{I}_0$ ,  $I_{0\max} = 1.5\bar{I}_0$ ,  $\omega_{ac} = 10^{-4}$ ,  $T = 0.05$ , and  $32 \times 32$  arrays. Other parameters as  $p = 7, 10, 15$ , and  $\Delta I_0 = 0.5, 1.5, 2$  were as well investigated. The full range of magnetic field was explored, from a single vortex to the fully frustrated case ( $f = 1/2$ ) in system with  $L = L_x = L_y = 32, 64, 100, 128$ .

**Results.**—In Fig. 1 we show mean dc voltage  $\langle V_{dc} \rangle$  vs the amplitude of the ac current  $I_{ac}$  for different vortex densities  $f$ . These results imply rectification: a net directional vortex motion parallel to the ratchet modulation in response to an alternating force. For low  $f$ ,  $\langle V_{dc} \rangle$  is maximum at an optimal value of  $I_{ac}$  and decreases slowly for larger  $I_{ac}$  as the ratchet potential is effectively washed out by the fast vortex motion. This behavior is qualitatively the one expected for a single particle rocking ratchet system [2]. Let us note, however, that even for highly diluted vortex systems the intensity of rectification is not additive: for example, with  $f = 1/32$  in a  $32 \times 32$  array we have 32 vortices but as we can see in Fig. 1 the response is  $\sim 12$  times, and not 32 times the response of one single vortex ( $f = 1/L^2$ ). This nonadditivity is even more pronounced for higher  $f$ . By increasing frustration from  $f = 1/32$  to  $f = 1/2$  the rectification peak presents both a reduction and a shift of the optimal  $I_{ac}$  value. A more intriguing feature appears when  $f$  is further increased. For  $0.17 \leq f < 1/2$  an inversion of the vortex flow direction is observed at small  $I_{ac}$  values and the window with  $\langle V_{dc} \rangle < 0$  becomes wider as  $f$  is increased. The nonmonotonic behavior observed as a function of  $f$  is a clear evidence that

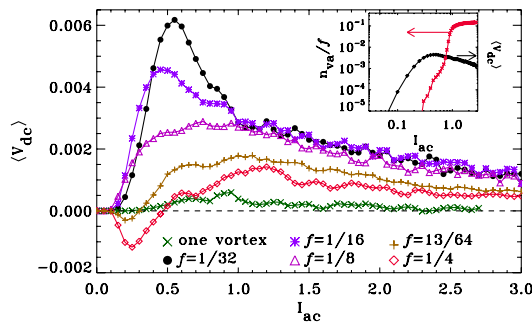


FIG. 1 (color online). Rectified vortex motion:  $I_{ac}$ - $V_{dc}$  characteristics examples increasing vortex density, from one vortex in the sample ( $f = 1/L^2$ ) towards  $f = 1/2$ . Inset:  $\langle V_{dc} \rangle$  vs  $I_{ac}$  for  $f = 1/32$ , in log-log scale (right y axis) and vortex-antivortex pairs density normalized by frustration,  $n_{va}/f$  (left y axis).

vortex-vortex interactions are relevant for the rectification effect at all  $f$ . On the other hand it is well known that the frustrated XY model, equivalent to our model for 2D JJA under an external  $H$  [14], can also present a finite density of thermally excited vortex-antivortex pairs,  $n_{va} = (\langle |b(\tilde{\mathbf{n}})| \rangle - f)/2$ , over the magnetic field induced vortex pattern. It is then important to understand its contribution to the ratchet effect. In the inset of Fig. 1 we plot both  $\langle V_{dc} \rangle$  and  $n_{va}/f$  vs  $I_{ac}$  for  $f = 1/32$ . We see that  $n_{va}$  increases monotonically and saturates to 10% of  $f$  at  $I_{ac} \sim 0.8$ . We find the same behavior for all  $f$  but the saturation value of  $n_{va}$  decreases with increasing  $f$ , being less than  $0.01f$  for  $f > 1/8$ . We conclude that the effect of pairs is almost negligible in the CR regime, but it is relevant for diluted vortex lattices at large applied currents and they must be considered to reproduce properly the experimental rectification tails.

A summary of our numerical results on voltage rectification vs vortex density is presented in Fig. 2 in comparison with experiments [15]. In Fig. 2(a) we show numerical curves for  $f = 1/4$  and  $f = 1 - f = 3/4$ . From the symmetries of the frustrated XY Hamiltonian:  $\mathcal{H}(f) = \mathcal{H}(-f) = \mathcal{H}(1 - f)$  [14], we expect symmetrical transport properties around  $f = 1/2$ . Since vortex and antivortex motion is rectified in the same direction we have  $\langle V_{dc} \rangle(f) = -\langle V_{dc} \rangle(1 - f)$ . This means that in the  $0 \leq f \leq 1/2$  range of magnetic field the dissipation arises from the motion of “positive” vortices while the flux of “negative” vortices (antivortices) yields dissipation in the  $1/2 \leq f \leq 1$  range. In Fig. 2(b) contour plots of  $\langle V_{dc} \rangle$  show the occurrence of voltage rectification in the  $I_{ac} - f$  plane. Current reversals occur only in the regime of strong vortex repulsion around  $f = 1/2$ , in a single interval,  $0.17 \leq f < 0.5$ . Comparing Figs. 2(b) and 2(c) we see a good qualitative agreement with experiments.

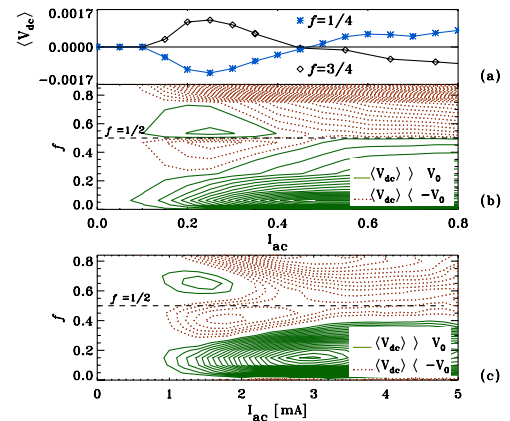


FIG. 2 (color online). (a)  $\langle V_{dc} \rangle$  vs  $I_{ac}$  for  $f = 1/4$  and  $f = 3/4$ . (b) Numerical  $\langle V_{dc} \rangle$  contour plots in  $I_{ac} - f$  plane at  $T = 0.05E_J/k_B$  and  $\omega_{ac} = 10^{-4}(1/\tau_J)$ . Red (or light gray) dotted lines represent  $\langle V_{dc} \rangle < -V_0$  and green (or gray) solid lines,  $\langle V_{dc} \rangle > V_0 = 5 \times 10^{-5}R_N I_0$ . (c) Experimental contours at  $T = 3.8$  K,  $\omega_{ac} = 1$  kHz and  $V_0 = 15$  nV (see [15]).

For applications it is also important to accurately determine the range of parameters where rectification would be observable. In Fig. 3(a) we see a well-defined saturation plateau for  $\langle V_{dc} \rangle$  at low frequencies. At high  $\omega_{ac}$  the fast changes in the potential slope do not allow vortices to adapt to the ratchet potential during a cycle. For all  $I_{ac}$  the mean voltage thus decays, becoming negligible at  $\omega_{ac} \gtrsim 0.01(\tau_J)^{-1}$ . Then we predict an observable rectification up to  $\sim 100$  kHz in good agreement with [15], if we use typical parameters,  $R_N = 0.01 \Omega$  and  $I_0 = 1 \mu A$ , to estimate our unit of frequency  $(\tau_J)^{-1} \sim 30$  MHz. Rectification can also depend on the parameters of the ratchet potential. In Fig. 3(b) we see that  $\langle V_{dc} \rangle$  monotonically increase with  $\Delta I_0$  for all  $I_{ac}$ , and the optimal rectification increase approximately linearly for  $1.5 \leq \Delta I_0 \leq 2$  (see inset) and for  $\Delta I_0 \sim 2$  inversion disappears [19]. We thus see that the ratchet effect could be experimentally improved up to 1 order of magnitude by modulating accordingly the Josephson couplings. On the other hand, we find that rectification has no appreciable changes for the experimental values  $p = 7, 10, 15$  nor sharp commensurability effects between  $f$  and  $p$ . We also analyze the range of temperature where rectification occurs and size effects. We find a wide range of applicability,  $0 \leq T \leq 0.4$ , what makes JJA advantageous and that the main characteristics of our results are almost size independent for  $L > 32$  [19].

To understand collective transport effects and, in particular, *current reversal*, we study vortex structures and spatial and temporal correlations. In Figs. 4(a) and 4(b) we show vorticity snapshots for  $f = 1/8, 3/4$  at  $I_{ac} = 0$  illustrating the competition between the ratchet potential, which induces a modulated vortex density, and the repulsive vortex-vortex interaction that favors a uniform vortex density. For all  $f$  we find that vortices organize in dense vortex walls strongly pinned at the sawtooth minima. Interestingly, when CR starts, the static vortex structure present an averaged number of vortices in the walls similar to a checkerboard pattern, i.e.,  $\langle n_{v/wall} \rangle \sim L_y/2$ . The degree of periodic order is reflected by the intensity of the peaks at  $\mathbf{k} = (n2\pi/p, 0)$  of the averaged vortex structure factor  $S(\mathbf{k}) = \langle |\frac{1}{L^2} \sum_{\tilde{\mathbf{n}}} b(\tilde{\mathbf{n}}) \exp(i\mathbf{k} \cdot \tilde{\mathbf{n}})|^2 \rangle$  shown in Fig. 4(c). A ring appears around the central peak representing the disordered structure observed in the interwall region, inside which the vortex density becomes more uniform as  $f$

approaches  $f = 1/2$  [compare  $\langle n_{v/c} \rangle$  in (a) vs (b)]. When the system is driven the ratchet-induced periodicity survives but its amplitude decays with increasing  $I_{ac}$ . We find that the degree of order decreases considerably for  $f$  around  $f = 1/2$  in the CR regime, although vortex walls at small  $I_{ac}$  are still well defined; see Fig. 4(d). We now analyze the instantaneous vortex dynamics. In Fig. 5 we show examples of typical voltage response vs time during a period at which its steady value  $\langle V_{dc} \rangle$  [see Fig. 2(a)] is already achieved. The amplitude of the almost symmetrical temporal oscillations around  $V_t = 0$  is much larger, 1 order of magnitude, than  $\langle V_{dc} \rangle$  for all  $I_{ac}$ . This implies that rectification arises from tiny differences between the two directions of motion and explains the low efficiency of the device and the need of very large  $\tau_{ac} = \omega_{ac}^{-1}$  to resolve the effect. The dc-limit analysis confirms this result [19]. Insets (a),(b) in Fig. 5 show  $b(\tilde{\mathbf{n}})$  snapshots at time  $[0, 0.25]\tau_{ac}$ , respectively. Most of the time the moving vortex lattice is highly disordered (as seen at  $t/\tau_{ac} = 0.25$ ), except for small forces close to depinning (as in  $t/\tau_{ac} \sim 0$ ) where the ratchet-induced periodicity is more visible. This fluctuating order produces the small peaks in the averaged structure factor shown in Fig. 4(d). In Fig. 5(c) voltage power spectrum for different vortex densities are analyzed. Time correlations appear clearly at  $\omega_{ac}$  and higher harmonics, as it is expected for one particle in a ratchet potential. Note, however, that interactions modify the harmonics structure, as it is seen comparing  $f = 3/4$  with more diluted vortex lattices,  $f = 1/8$  and  $f = 1/16$  where more harmonic peaks appear. We thus see that temporal order is only determined by the ac drive as it is ex-

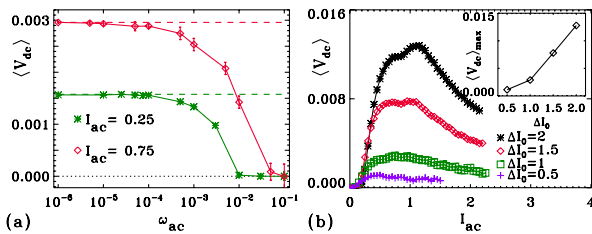


FIG. 3 (color online). Rectification dependences for  $f = 1/8$ : (a) On  $\omega_{ac}$ : at  $I_{ac} = 0.25$  ( $\star$ ) and  $I_{ac} = 0.75$  ( $\diamond$ ) ( $\langle V_{dc} \rangle_{\max}$ , see Fig. 1). (b) On pinning potential:  $\langle V_{dc} \rangle - I_{ac}$  vs  $\Delta I_0$ . Inset:  $\langle V_{dc} \rangle_{\max}$  vs  $\Delta I_0$ .

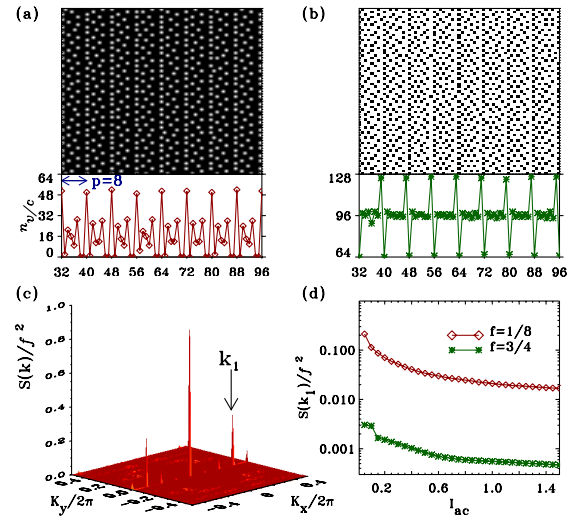


FIG. 4 (color online). Vortex structures: static  $b(\tilde{\mathbf{n}})$  obtained quenching from high  $T$  towards  $T = 0$  ( $L = 128$  but a fraction is shown for transparency). Vortices are white plaquettes). In (a)  $f = 1/8$  and (b)  $f = 3/4$ , both with  $\langle n_{v/c} \rangle$  below, the number of vortices per column. (c)  $S(\mathbf{k})/f^2$  corresponding to  $b(\tilde{\mathbf{n}})$  in (a) with clear peaks due to the ratchet potential, as  $k_1$ . (d)  $S(k_1)/f^2$  vs  $I_{ac}$  for  $f = 1/8, 3/4$  at  $T = 0.05$  and  $\omega_{ac} = 10^{-4}$ .

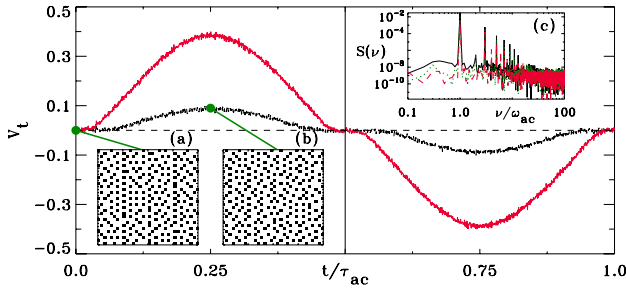


FIG. 5 (color online). Time voltage response to an ac drive of  $I_{ac} = 0.3$  for  $f = 3/4$  (smaller amplitude curve, black line), with  $\langle V_{dc} \rangle > 0$  and  $I_{ac} = 0.7$  [larger amplitude, red (or light gray) line], with  $\langle V_{dc} \rangle < 0$ . Insets (a),(b): instantaneous vorticity for  $I_{ac} = 0.3$  and  $t/\tau_{ac} = 0, 0.25$  respectively. (c) Power spectrum for  $f = 3/4$  (solid black line),  $f = 1/8$  [dotted green (or gray) line] and  $f = 1/16$  (dashed red line).

pected for vortices moving incoherently. No trace of a washboard frequency is observed for any  $f$  nor  $I_{ac}$ . Therefore no dynamical phase transitions are induced by the ac drive and the system behaves as a modulated driven plasma.

*Discussion.*—Our results present some similarities but also some marked differences with other 2D vortex ratchet systems. First, let us note that inverted rectification appears *only at low drives within a single range of high  $f$  around  $f = 1/2$*  (Fig. 2). This is similar to CR observed in arrays of dots in SC films by Villegas *et al.* [7], but their explanation based on interstitial vortices moving over an inverted ratchet potential, is not suitable for JJA as interstitial cannot be defined. Our results are also different to the multiple CRs observed and explained by de Souza Silva *et al.* in SC films with antidots arrays [7]. The differences can be attributed to the strong pinning generated by dots or antidots, which can localize a few vortices in very small regions and produce a very coherent individual motion. In our case an extended weak potential pins and deforms collectively the vortex density although individual vortex motion remains highly incoherent. In addition, underdamped dynamics was also shown to provide CR [7]. In our case no evidence of an effective dynamically induced inertia is found, however, as no hysteresis in Fig. 1, nor out of phase voltage response is observed, Fig. 5. CR in JJA thus presents novel features deserving discussion.

Since CR is observed near the onset of dissipation, an analysis of the asymmetric depinning is useful. In the absence of vortex interactions it is clear that the critical current in the easy direction of the ratchet potential,  $I_{dep}^{easy} \sim \Delta U/(p-1)$  is smaller than the one in the hard direction  $I_{dep}^{hard} \sim \Delta U$ . Therefore the onset of rectification occurs when  $I_{ac} \sim I_{dep}^{easy}$  with a net motion in the easy direction. In the presence of interactions the situation can be rather different [7], since vortices tend to screen the ratchet potential thus modifying the critical currents and mobility of single vortex excitations in each direction differently. It is clear that a small tilt of the ratchet potential in the hard direction produces well-defined walls with a high vortex

density at the local minima of the sawtooth. On the contrary, a tilt in the easy direction favors a smoother vortex density profile. Calculating the force exerted on a vortex by a periodic array of vortex walls we can easily show that  $I_{dep}^{hard}$  is reduced by an amount proportional to the vortex density at the walls,  $\tilde{I}_{dep}^{hard} = \Delta U - \alpha f_{wall}$ , while in the easy direction  $I_{dep}^{easy}$  remains unchanged. Hence, CR can occur above a critical vortex density  $f_c$  such that  $\tilde{I}_{dep}^{hard} = I_{dep}^{easy}$  at  $f_c$ , yielding  $f_c \sim \frac{\Delta U}{\alpha} \left( \frac{p-2}{p-1} \right)$ . This simple argument is consistent with the fact that inversion is observed at high  $f$ , disappears with increasing  $\Delta U$ , and is weakly dependent on  $p$  (details and dc limit confirming this scenario in [19]). At larger  $I_{ac}$  the dynamical smoothing of the vortex density reduces the screening and the easy direction for rectification is recovered. Figure 1 shows that this recovering occurs at higher  $I_{ac}$  for higher  $f$ , consistent with the existence of denser walls at high  $f$ . Our results thus show that vortex-vortex interactions can overscreen the asymmetry of the ratchet potential as was noted in [7] but the mechanism is *purely collective*, since individual vortex motion is highly incoherent as in a driven modulated fluid. Indeed, this effect could be relevant for a wide family of interacting many-body ratchet systems [19].

I acknowledge useful discussions with P. Martinoli, A. B. Kolton, D. Domínguez, D. E. Shalóm (also for providing experimental data), H. Pastoriza, and H. Beck. This work was supported by the Swiss NSF.

- [1] F. Jülicher *et al.*, Rev. Mod. Phys. **69**, 1269 (1997).
- [2] P. Reimann, Phys. Rep. **361**, 57 (2002).
- [3] G. I. Menon, Physica (Amsterdam) **372A**, 96 (2006).
- [4] R. D. Astumian and P. Hänggi, Phys. Today **55**, No. 11, 33 (2002).
- [5] H. Linke (Ed.), Appl. Phys. A **75**, No. 2, 167–352 (2002).
- [6] C. S. Lee *et al.*, Nature (London) **400**, 337 (1999).
- [7] J. E. Villegas *et al.*, Science **302**, 1188 (2003); C. C. de Souza Silva *et al.*, Phys. Rev. B **73**, 014507 (2006); Nature (London) **440**, 651 (2006), and references therein.
- [8] D. Cole *et al.*, Nat. Mater. **5**, 305 (2006).
- [9] I. Zapata *et al.*, Phys. Rev. Lett. **77**, 2292 (1996).
- [10] F. Falo *et al.*, Europhys. Lett. **45**, 700 (1999).
- [11] E. Trías *et al.*, Phys. Rev. E **61**, 2257 (2000).
- [12] M. Beck *et al.*, Phys. Rev. Lett. **95**, 090603 (2005).
- [13] J. B. Majer *et al.*, Phys. Rev. Lett. **90**, 056802 (2003).
- [14] See M. Tinkham, *Introduction to Superconductivity* (McGraw-Hill, Inc., New York, 1996); R. S. Newrock *et al.*, Solid State Phys. **54**, 263 (2000), and references therein.
- [15] D. E. Shalóm and H. Pastoriza, Phys. Rev. Lett. **94**, 177001 (2005).
- [16] K. K. Mon and S. Teitel, Phys. Rev. Lett. **62**, 673 (1989); J. S. Chung *et al.*, Phys. Rev. B **40**, 6570 (1989).
- [17] V. I. Marconi and D. Domínguez, Phys. Rev. B **63**, 174509 (2001).
- [18] D. Domínguez and J. V. José, Phys. Rev. B **53**, 11692 (1996).
- [19] V. I. Marconi *et al.* (to be published).